

# Regulation of cAMP-dependent Protein Kinases

## THE HUMAN PROTEIN KINASE X (PrKX) REVEALS THE ROLE OF THE CATALYTIC SUBUNIT $\alpha$ H- $\alpha$ I LOOP<sup>\*[5]</sup>

Received for publication, June 23, 2010, and in revised form, August 10, 2010 Published, JBC Papers in Press, September 6, 2010, DOI 10.1074/jbc.M110.155150

Mandy Diskar<sup>‡1,2</sup>, Hans-Michael Zenn<sup>‡1</sup>, Alexandra Kaupisch<sup>‡</sup>, Melanie Kaufholz<sup>‡</sup>, Stefanie Brockmeyer<sup>‡</sup>, Daniel Sohmen<sup>§</sup>, Marco Berrera<sup>¶</sup>, Manuela Zaccolo<sup>¶3</sup>, Michael Boshart<sup>§</sup>, Friedrich W. Herberg<sup>‡</sup>, and Anke Prinz<sup>‡4</sup>

From the <sup>‡</sup>Department of Biochemistry, University of Kassel, Heinrich-Plett-Strasse 40, 34132 Kassel, Germany, the <sup>§</sup>Biocenter, Section Genetics, University of Munich (LMU), Großhaderner Strasse 2-4, 82152 Planegg-Martinsried, Germany, and the <sup>¶</sup>University of Glasgow, University Avenue, Glasgow G12 8QQ, Scotland, United Kingdom

cAMP-dependent protein kinases are reversibly complexed with any of the four isoforms of regulatory (R) subunits, which contain either a substrate or a pseudosubstrate autoinhibitory domain. The human protein kinase X (PrKX) is an exemption as it is inhibited only by pseudosubstrate inhibitors, *i.e.* RI $\alpha$  or RI $\beta$  but not by substrate inhibitors RII $\alpha$  or RII $\beta$ . Detailed examination of the capacity of five PrKX-like kinases ranging from human to protozoa (*Trypanosoma brucei*) to form holoenzymes with human R subunits in living cells shows that this preference for pseudosubstrate inhibitors is evolutionarily conserved. To elucidate the molecular basis of this inhibitory pattern, we applied bioluminescence resonance energy transfer and surface plasmon resonance in combination with site-directed mutagenesis. We observed that the conserved  $\alpha$ H- $\alpha$ I loop residue Arg-283 in PrKX is crucial for its RI over RII preference, as a R283L mutant was able to form a holoenzyme complex with wild type RII subunits. Changing the corresponding  $\alpha$ H- $\alpha$ I loop residue in PKA C $\alpha$  (L277R), significantly destabilized holoenzyme complexes *in vitro*, as cAMP-mediated holoenzyme activation was facilitated by a factor of 2–4, and lead to a decreased affinity of the mutant C subunit for R subunits, significantly affecting RII containing holoenzymes.

The protein kinase A (PKA) holoenzyme is a heterotetramer composed of two catalytic (C)<sup>5</sup> subunits kept inactive by a

dimer of R subunits. Each R subunit monomer contains two tandem cAMP-binding domains, in which the sequential binding of two cAMP molecules releases an active C subunit (1). Two main classes of PKA isozymes, type I and type II, distinguishable by their R subunits, have been described. Crystal structures and solution scattering data provide evidence of a complex interaction network between C and R subunits as well as differences in global structure of PKA type I and type II holoenzymes (2–5).

*Homo sapiens* express the PKA R subunit isoforms RI $\alpha$ , RI $\beta$ , RII $\alpha$ , and RII $\beta$  and C subunits C $\alpha$ , C $\beta$ , and C $\gamma$ . Another cAMP-dependent protein kinase is PrKX and possibly protein kinase Y (PrKY). PrKY is 94% homologous to PrKX, but shortened by 81 amino acids at the C terminus. On the genome level, *PRKX* and *PRKY* are implicated in sex-reversal disorders (6). PrKX is being discussed as a phylogenetically and functionally separate enzyme (7, 8). In contrast to the ubiquitously expressed C $\alpha$  subunit, PrKX is mainly active during embryonic organ development and cellular differentiation in hematopoietic lineages. It was found to be crucial for macrophage and granulocyte maturation (9, 10). PrKX was shown to be involved in renal development, regulating epithelial cell migration, ureteric bud branching, and induction of glomeruli formation (8, 11–13).

C $\alpha$  and human PrKX differ by their selective holoenzyme formation in living cells, as PrKX is inhibited only by RI $\alpha$ , but not by RII $\alpha$  (14, 15). Here, we have tested all four human R subunits for the first time side by side and show that this so far unique property of RI over RII preference with respect to autoinhibition appears to be an evolutionarily conserved feature of PrKX and at least four of its orthologs (*Mus musculus* Pkare, *Drosophila melanogaster* DC2, *Trypanosoma brucei* PKAC3, human PrKY), and possibly also *Caenorhabditis elegans* F47F2.1b.

Previously, we identified the R subunit autoinhibitory site as a main determinant for isoform-specific regulation of PKA (15). We were able to gain significant binding of PrKX with RII $\alpha$  solely by mutation of Ser-99 to Ala in the RII $\alpha$  autoinhibitory domain (P<sup>0</sup>-site). Conversely, introducing an autophosphorylation site Ser or an Asp in the inhibitory domain of RI $\alpha$  completely abolished binding to PrKX, but not to C $\alpha$ . This led us to believe that at least one peripheral interaction interface could be non-functional in PrKX holoenzymes when compared with the C $\alpha$  holoenzymes. We therefore set out to pinpoint this position in PrKX, applying mainly BRET-based cell interaction

\* This work was supported, in whole or in part, by National Institutes of Health Grant R01 AA18060 from the National Science Foundation-NIH Collaborative Research in Computational Neuroscience Program (to M. Z.), European Union Grant LSHB-CT-2006-037189 (to F. W. H. and M. Z.), Bundesministerium für Bildung und Forschung NGFN2 Grant FKZ01GR0441 (to F. W. H.), and Deutsche Forschungsgemeinschaft BO1100/2 (to M. B.).

[5] The on-line version of this article (available at <http://www.jbc.org>) contains supplemental Figs. S1 and S2 and Tables S1 and S2.

<sup>1</sup> Both authors contributed equally to this work.

<sup>2</sup> Supported by a Ph.D. grant of the Otto-Braun fonds of the University of Kassel.

<sup>3</sup> Supported by Fondation Leducq Grant O6 CVD 02 and British Heart Foundation Grant PG/07/091/23698.

<sup>4</sup> To whom correspondence should be addressed: Dept. of Biochemistry, University of Kassel, Heinrich-Plett-Str. 40, 34132 Kassel, Germany. Tel.: 49-561-8044239; Fax: 49-561-8044466; E-mail: ankeprinz@uni-kassel.de.

<sup>5</sup> The abbreviations used are: C, PKA catalytic subunit; BRET, bioluminescence resonance energy transfer; IBMX, 3-isobutyl-1-methylxanthine; MD, molecular dynamics; PKA, cAMP-dependent protein kinase A; R, PKA regulatory subunit; Rluc, *Renilla* luciferase; PrKX, protein kinase X; PrKY, protein kinase Y; SPR, surface plasmon resonance; NTA, nitrilotriacetic acid.

assays and SPR analyses with wild type and mutant C subunits. Our investigations led to the identification of residue Arg-283, located in the PrKX  $\alpha$ H- $\alpha$ I loop, as important for the differential regulation of the PrKX subfamily, *i.e.* its selective autoinhibition by RI subunits in living cells. Supported by biochemical and modeling evidence we provide evidence that an Arg at position 283 in PrKX or at position 277 in the mutant C $\alpha$  interferes with holoenzyme stability and allosteric regulation of the kinases by disturbing a crucial interaction platform composed of activation loop (C subunit) and  $\alpha$ A-helix (R subunit) residues.

## EXPERIMENTAL PROCEDURES

**Protein Expression Vectors**—The oligonucleotides and vectors used for cloning of prokaryotic and eukaryotic expression vectors and for subsequent site-directed mutagenesis using the QuikChange mutagenesis kit (Stratagene) are provided under [supplemental Table S2](#). Cloning of human *PRKARIA*, *PRKAR2A*, *PRKACA*, and *PRKX* genes into the BRET vectors was published previously (15, 16). Mutagenesis of PrKX was performed using plasmid pFastBac HTb-*PRKX* (15) as the template. For protein purification, human C $\alpha$  was subcloned into pHis5BA via pRSET<sub>B</sub>-hC $\alpha$  ([supplemental Table S2](#)). *Pkare* was amplified from pCMVSPORT6-*Pkare* (RZPD, Berlin, Germany). *PRKY* was amplified from cDNA clone pCMV6-XL5-*PRKY* (accession number NM\_002760.2) purchased from OriGene (Rockville, MD). *C. elegans F47F2.1b* was amplified from pDONR201-*F47F2.1b*, provided by Dr. M. Jedrusik-Bode, MPI for Biophysical Chemistry, Göttingen, Germany. A DC2 cDNA clone (FlyBase clone number AT10577) was obtained from the Drosophila Genomics Resource Center (Bloomington, IN). The full-length clone and a 1–227 deletion variant were amplified and each subcloned into GFP<sup>2</sup>-C2. The *T. brucei* PKAC3 coding region (UniProt accession number Q388U5)<sup>6</sup> was amplified to allow subcloning into GFP<sup>2</sup>-C3.

Plasmids for expression of R subunits RI $\alpha$  (pRSET<sub>B</sub>-*PRKA1A*) and RII $\alpha$  (pRSET<sub>B</sub>-*PRKA2A*) were a kind gift from Prof. Dr. S. S. Taylor, University of California, San Diego. pRSET<sub>B</sub>-*PRKA1B* and Rluc(h)-N2-*PRKA1B* were subcloned from pBluescript-*PRKA1B*, a gift of Prof. Dr. K. Tasken, University of Oslo, Norway. The human *PRKA2B* coding region was amplified from a cDNA clone (OriGene, accession number NM\_002736.2) and subcloned in Rluc(h)-N2 and pRSET<sub>B</sub>, respectively. Point mutations of C $\alpha$ , PrKX, *F47F2.1b*, PKAC3, RI $\beta$ , and RII $\beta$  were introduced using the oligonucleotides listed under [supplemental Table S2](#). Mutagenesis of RI $\alpha$  and RII $\alpha$  was published previously (15). All plasmids used in this study were sequence verified.

**BRET Assays**—COS-7 cells (ATCC CRL-1651) were transfected in white 96-well microplates (Nunc) as described before (17) using 0.25  $\mu$ g of DNA per plasmid and well. Two days after transfection, cells were rinsed with glucose-supplemented Dulbecco's PBS (D-PBS, Invitrogen), and treated with forskolin (50  $\mu$ M) and 3-isobutyl-1-methylxanthine (IBMX) (500  $\mu$ M) at final concentrations in D-PBS for 20 min. Coelenterazine 400a (Biotrend) was added immediately before BRET read-out. The

light output was taken consecutively (read time 1 s, gain 25) for each well with filters at 410 nm wavelength ( $\pm$ 80 nm band pass) for the *Renilla* luciferase (Rluc) and 515 nm ( $\pm$ 30 nm band pass) for the GFP<sup>2</sup> emission using an  $\alpha$ -fusion microplate reader (PerkinElmer Life Sciences). Wells containing cells expressing Rluc alone were included in every experiment (background BRET signal, bg). Emission values (em) obtained with untransfected (n.t.) cells were subtracted, and BRET ratios were calculated as follows:  $(em_{515\text{ nm}} - \text{n.t. cells}_{515\text{ nm}})/(em_{410\text{ nm}} - \text{n.t. cells}_{410\text{ nm}})$ . In general, experiments were repeated at least three times with six wells per experimental condition. Average results are represented as mean  $\pm$  S.E. Statistical evaluation (one-way analysis of variance with Newman-Keuls post tests) was carried out with the GraphPad Prism software version 4.0 (GraphPad).

**Protein Expression and Purification**—Expression and affinity purification of R subunits was carried out as described (18, 19). His<sub>6</sub>-tagged human C $\alpha$  (His<sub>6</sub>-C $\alpha$ ) and His<sub>6</sub>-C $\alpha$ <sub>L277R</sub> were expressed overnight at room temperature in *Escherichia coli* BL21(DE3) (Novagen) and purified using a Talon affinity resin and standard conditions (Clontech). Expression and purification of His<sub>6</sub>-PrKX and His<sub>6</sub>-PrKX<sub>R283L</sub> was performed as described (15).

**Spectrophotometric Kinase Activity Assay**—The specific activity of the recombinant PKA C $\alpha$  was tested by the continuous enzyme-linked spectrophotometric method described by Cook *et al.* (20) using 260  $\mu$ M of the synthetic substrate Kemptide (LRRASLG; Biosynthan). 1 Unit/mg is defined as 1  $\mu$ mol  $\times$  min<sup>-1</sup>  $\times$  mg<sup>-1</sup>. Apparent activation constants ( $K_{\text{act}}$ ) were determined with 10 or 20 nM reconstituted holoenzyme by adding varying concentrations of cAMP in assay buffer containing 1 mM ATP and 10 mM MgCl<sub>2</sub> (15).

**Surface Plasmon Resonance**—Methods for interaction analyses of C $\alpha$  and PrKX with R subunits were published previously (15). Briefly, 200–300 resonance units (RU) of His<sub>6</sub>-C $\alpha$ , His<sub>6</sub>-C $\alpha$ <sub>L277R</sub>, His<sub>6</sub>-PrKX, and His<sub>6</sub>-PrKX<sub>R283L</sub> were covalently coupled on a modified Ni<sup>2+</sup>-nitrilotriacetic acid (NTA) chip via primary amines. A dilution series (0.5 to 256 nM R subunit) was injected at a flow rate of 30  $\mu$ l/min, and association and dissociation were recorded for 5 min each. A blank NTA surface was used as the control surface. Additionally, an injection of buffer (20 mM HEPES, pH 7.4, 150 mM NaCl, 0.005% Tween 20, 50  $\mu$ M EDTA, 1 mM ATP, and 10 mM MgCl<sub>2</sub>) was subtracted from each sensorgram. Surface regeneration was achieved by injecting 100  $\mu$ M cAMP and 2.5 mM EDTA, diluted in running buffer. The rate constants for association ( $k_a$ ) and dissociation ( $k_d$ ) were fitted assuming a 1:1 Langmuir binding model using Biaevaluation 4.1 (Biacore AB). Equilibrium binding constants ( $K_D$ ) were calculated by dividing  $k_d$  with  $k_a$ .

**Molecular Dynamics (MD) Simulations**—The structural models of C $\alpha$  and C $\alpha$ <sub>L277R</sub> in complex with the bovine (b) RII $\alpha$  were based on the available x-ray structures solved at 2.5 Å of resolution (Protein Data Bank code 2QVS (4)). The L277R mutant side chain was modeled to maintain the orientation of the wild type side chain in the experimental structures. Missing atoms were added assuming standard bond lengths and angles. The models were immersed in parallel piped water boxes, whose edges were  $\sim$ 9, 10, and 12 nm; sodium or chlorine ions

<sup>6</sup> M. Boshart, unpublished data.

## Intracellular PKA Holoenzyme Regulation

were added to neutralize the boxes. MD simulations were performed using the computational setup already applied before (21, 22), whose main properties are: the MD program Gromacs was employed (23), using the Amber99 force field for protein and TIP3P for water (24, 25), Lincs algorithm to constrain bonds (26), periodic boundary conditions, 10 Å cutoff for short range electrostatic and van der Waals interactions, particle mesh Ewald to treat long range electrostatics (27), and 2-fs integration time step. After energy minimization, 300 ps of MD of the solvent with gradual heating of the systems, the complexes underwent 14 ns of MD in the NPT ensemble at 300 K and 1 atm pressure, using the Berendsen thermostat and barostat (28). Root mean square deviations were calculated on  $\alpha$ -carbon atoms using the initial conformation as reference. Solvent accessible surfaces are calculated for the residues of the four complexes using the center-probe area definition (29), as in Ref. 30, and averaged over the second halves of the MD trajectories.

### RESULTS

**Inhibition of PrKX and Orthologs by Human R Subunits**—Previous *in vitro* and BRET-based interaction analyses in living cells using RI $\alpha$  and RII $\alpha$  subunits identified human PrKX as a type I $\alpha$ -specific PKA-like kinase (14, 15). To study binding patterns of PrKX-like kinases, we investigated binding of all four human R isoforms to PrKX, human PrKY, murine Pkare (31, 32), *D. melanogaster* DC2 (33), and a putative PrKX homolog from the protozoan parasite *T. brucei* (PKAC3, GenBank accession number AF253418 (34)).<sup>6</sup> They were all cloned as N-terminal GFP<sup>2</sup> fusions for eukaryotic protein expression. In analogy to the previously published protein expression constructs for human RI $\alpha$  and RII $\alpha$  (16), *Renilla* luciferase (Rluc) was genetically fused to the C terminus of RI $\beta$  and RII $\beta$ .

For BRET analyses in COS-7 cells, the five investigated PrKX-type kinase fusion constructs were co-transfected with each of the four human R subunits at a 1:1 ratio of plasmid DNA. Employing this BRET assay, a signal above the background indicates PKA holoenzyme formation, which can be reduced by increasing intracellular cAMP ([cAMP]<sub>i</sub>). Furthermore, the BRET signal of a given interaction pair provides a quantitative measure of the amount of holoenzyme present in resting *versus* stimulated cell populations (17). Fig. 1 shows the protein-protein interaction analyses, where PrKX (A), PrKY (B), Pkare (C), a deletion variant of DC2 ( $\delta 1-227$ ,  $\Delta$ DC2) (D) and PKAC3 (E) were each probed by BRET for binding to the four human R subunits. With DC2 we achieved BRET signals only with the N-terminal deletion variant, but not the wild type protein (data not shown). The BRET analyses revealed that PrKX, Pkare,  $\Delta$ DC2, and PKAC3 displayed very similar R subunit binding patterns, interacting specifically only with RI $\alpha$  and RI $\beta$ . In all cases, we observed the highest overall BRET values when RI $\beta$  was co-expressed with the C subunits. PrKY (Fig. 1B) binds only to RI $\beta$  resulting in a BRET signal of about 30% of the PrKX:RI $\beta$  signal (compare Fig. 1, A and B). Binding of RI to the C subunits was reduced by  $\sim$ 50% upon treatment with 50  $\mu$ M forskolin and 500  $\mu$ M IBMX, which we used to get to a sustained increase of [cAMP]<sub>i</sub>, in agreement with previous results (Fig. 1) (15). Independent investigations showed that (local) substrate availability greatly enhances the sensitivity of PKA type I $\alpha$

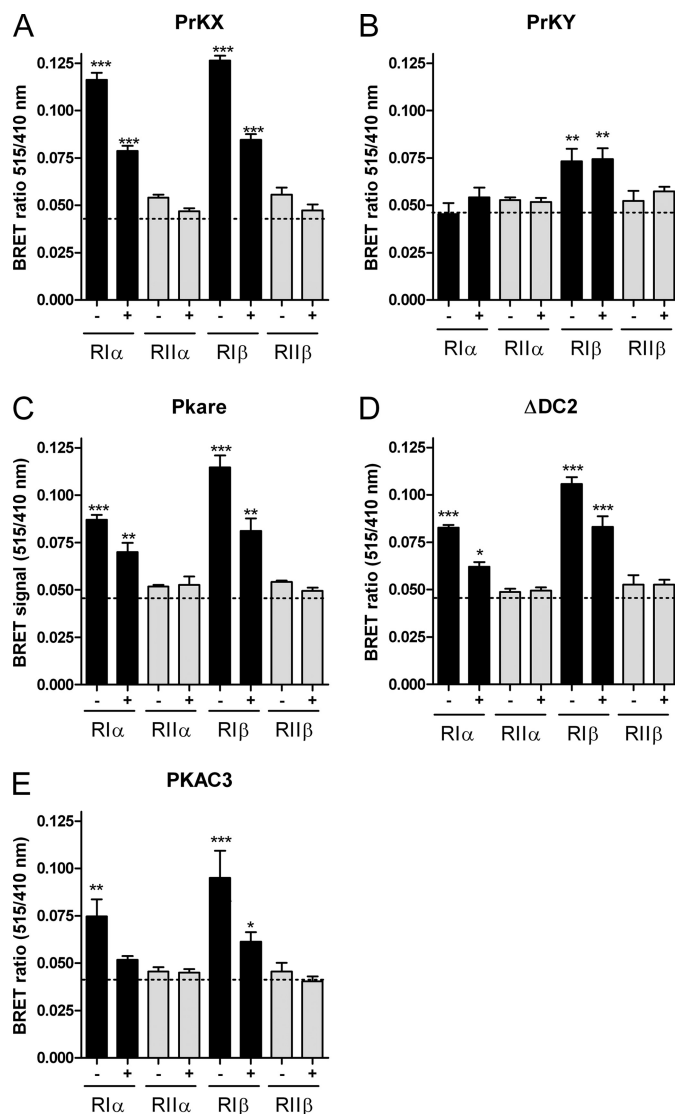


**FIGURE 1. PKA RI-specific interaction of PrKX-like kinases is conserved between species.** To follow PKA subunit interaction in living cells, PrKX (A), PrKY (B), Pkare (C),  $\Delta$ DC2 (D), and PKAC3 (E) were each fused N-terminally with GFP<sup>2</sup>. RI $\alpha$ , RII $\alpha$ , RI $\beta$ , and RII $\beta$  were cloned into eukaryotic vectors fusing them C-terminally with *Renilla* luciferase (Rluc). For BRET experiments, COS-7 cells were co-transfected with the indicated constructs and grown for 2 days prior to the incubation with vehicle (–) or with (+) 50  $\mu$ M forskolin, 500  $\mu$ M IBMX dissolved in Dulbecco's PBS. BRET was measured immediately after addition of the luciferase substrate. Values are given as mean  $\pm$  S.E. of at least three independent experiments, each performed with  $n = 6$  replicates (\*\*\*,  $p < 0.001$ ; \*\*,  $p < 0.01$ ; \*,  $p < 0.05$ ). The dotted line indicates the mean background value.

toward [cAMP]<sub>i</sub> (35, 36). In contrast, the PrKY/RI $\beta$  interaction was not influenced by [cAMP]<sub>i</sub> (Fig. 1B), indicating that not only R subunit docking, but also its release could be hampered in PrKY. This result suggests that PrKY is lacking R interaction interface(s). In contrast to PrKX, we did not detect BRET with PrKY and any of the human isoforms of the heat stable protein kinase inhibitor (PKI (37) (data not shown). Attempts to purify active His<sub>6</sub>-PrKY after heterologous expression in Sf9 cells were also unsuccessful. We can therefore conclude that the C-terminal deletion of the kinase, which includes the last domain of the conserved catalytic core (subdomain 11) (38), likely leads to the expression of an inactive enzyme with a significantly diminished binding of substrates and pseudosubstrates.

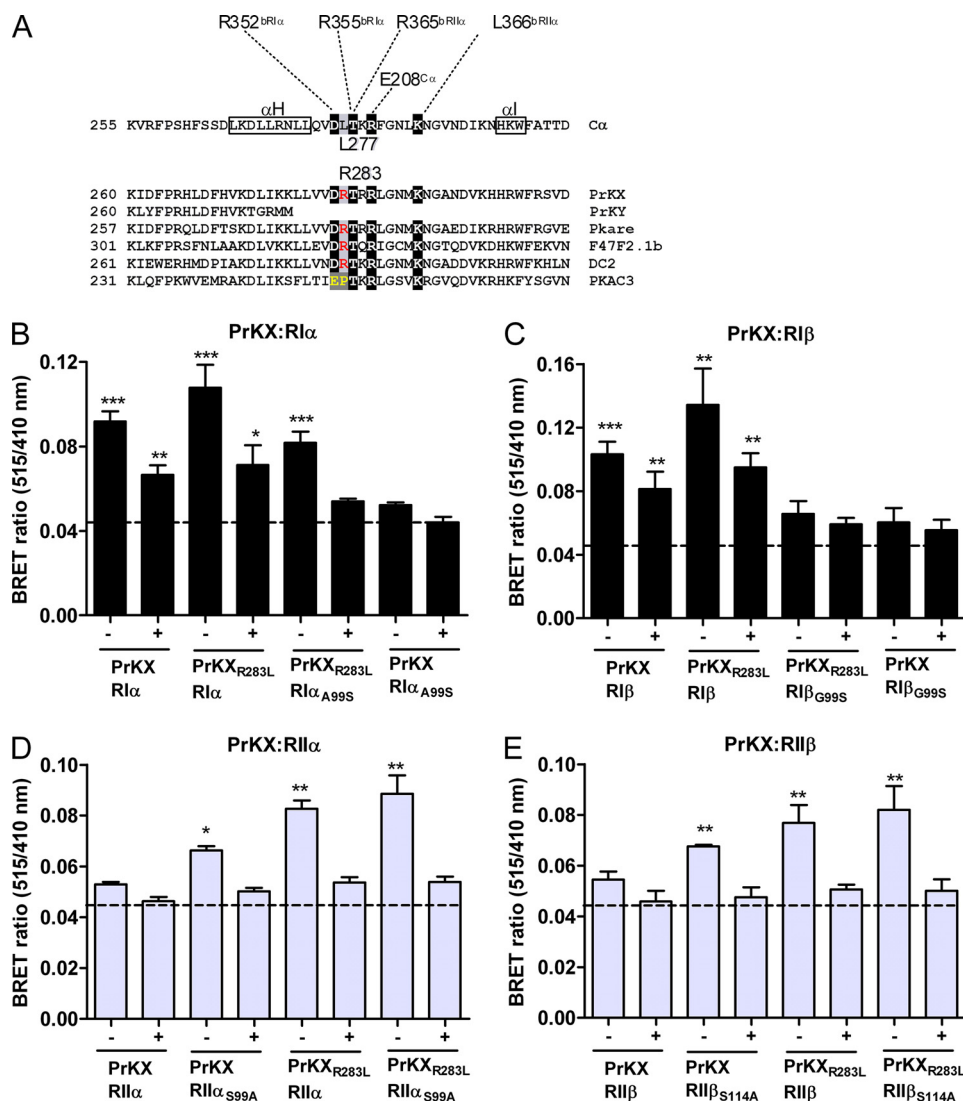


**FIGURE 2. Mutant PrKX (R283L) has the capacity for holoenzyme formation with RII subunits.** *A*, this partial alignment of the  $\alpha$ H- $\alpha$ I loop region of C $\alpha$  and PrKX-like kinases highlights the conserved C $\alpha$  residues previously found to be involved in bRI $\alpha$  (R352, R355) and bRII $\alpha$  (R365, L366) subunit coordination as well as intramolecular stabilization of C $\alpha$  (E208<sup>C $\alpha$</sup> ), all shaded in black. Non-conserved and/or experimentally addressed residues in this study are shaded gray and written in black (L277<sup>C $\alpha$</sup> ), red (R283<sup>PrKX</sup>, R280<sup>Pkare</sup>, R324<sup>F47F2.1b</sup>, R510<sup>DC2</sup>), and yellow (P254<sup>PKAC3</sup>, E253<sup>PKAC3</sup>). *B*, BRET interaction analyses of wild type and PrKX<sub>R283L</sub> with wild type or P<sup>0</sup>-site mutant R subunits were carried out as detailed in the legend to Fig. 1. Plasmids coding for GFP<sup>2</sup>-PrKX and GFP<sup>2</sup>-PrKX<sub>R283L</sub> were co-transfected with constructs expressing either RI $\alpha$ -Rluc or RI $\alpha$ <sub>A99S</sub>-Rluc (*C*), as in *B*, co-transfected with either RI $\beta$ -Rluc or RI $\beta$ <sub>G99S</sub>-Rluc constructs. *D*, as in *B*, combined with either RII $\alpha$ -Rluc or RII $\alpha$ <sub>S99A</sub>-Rluc. *E*, as in *B*, combined with either RII $\beta$ -Rluc or RII $\beta$ <sub>S114A</sub>-Rluc. Depicted are original BRET values (mean  $\pm$  S.E.) obtained from at least three independent repeats ( $n = 6$  wells; \*\*\*,  $p < 0.001$ ; \*\*,  $p < 0.01$ ; \*,  $p < 0.05$ ). + indicates treatment with forskolin/IBMX, - indicates mock treatment, and the dotted line represents the mean background value.

In contrast to PrKX and PrKX-like kinases, human C $\alpha$ , C $\beta$ 1, C $\beta$ 2, and C $\alpha$ s interact with all four human R subunits based on BRET (15, 16).<sup>7</sup> Thus, data provided here support an RI selective holoenzyme formation as a main characteristic of PrKX and four of its orthologs.

**Influence of the  $\alpha$ H- $\alpha$ I Loop of C $\alpha$  and PrKX on Differential R Subunit Binding**—To investigate inhibition of PrKX and conventional PKA C subunits in more detail, we aligned the sequences of the PKA-related kinase subfamilies and subjected them to phylogenetic analysis (supplemental Figs. S1, A–C, and

Table S1). From x-ray structural analysis of either RI $\alpha$  or RII $\alpha$  in complex with the C $\alpha$  subunit, the  $\alpha$ H- $\alpha$ I loop region of the C subunit was proposed to be important particularly for binding of the RII $\alpha$  subunit (3, 4). Residues Asp-276<sup>C $\alpha$</sup>  and Thr-278<sup>C $\alpha$</sup>  as well as the residues Thr-278<sup>C $\alpha$</sup>  and Lys-285<sup>C $\alpha$</sup>  were previously found to interact with the cAMP binding domain A of bovine RI $\alpha$  (Arg-352, Arg-355) and bovine RII $\alpha$  (Arg-365, Leu-266) subunits (Fig. 2A). These  $\alpha$ H- $\alpha$ I loop residues are conserved between PKA and PrKX-like kinases. To elucidate residues necessary for the interaction with RII subunits, we first mutated Lys-285 to Ala in C $\alpha$  and monitored holoenzyme formation using the BRET assay. This mutation had no effect on C subunit binding to any of the four human R subunits (data not shown), in agreement with a previous study investigating a Lys-285 to Pro mutant (39), suggesting a backbone rather than a side chain interaction between Lys-285<sup>C $\alpha$</sup>  and Leu-366<sup>bRII $\alpha$</sup> .

We then focused on a  $\alpha$ H- $\alpha$ I loop residue that differs between PrKX and C $\alpha$ , Arg-283<sup>PrKX</sup> and Leu-277<sup>C $\alpha$</sup> . Arg-283<sup>PrKX</sup> is conserved in all but one of the PrKX-like kinases investigated in this study and the corresponding residue Leu-277<sup>C $\alpha$</sup>  is common to C $\alpha$  and -orthologs (Fig. 2A and supplemental Fig. S1, B and C). We went on to replace Arg-283<sup>PrKX</sup> by Leu in PrKX and investigated the mutant protein for specific activity, intracellular and *in vitro* binding to wild type and P<sup>0</sup>-site mutant R subunits. The activities of the purified PrKX proteins were tested with a coupled spectrophotometric assay using the synthetic substrate Kempptide (LRRASLG) (20). Results were almost identical for PrKX (14) and mutant PrKX<sub>R283L</sub> ( $1.4 \pm 0.2$  units/mg, data not shown).

As depicted in Fig. 2, *D* and *E*, changing Arg-283<sup>PrKX</sup> to Leu had a significant stabilizing effect on wild type RII $\alpha$  and RII $\beta$  subunit binding in living cells. SPR analyses using the corresponding purified proteins lead to an about 10–12-fold increase in binding affinity of PrKX to RII $\alpha$  subunits (Table 1 and Fig. 3, *C* and *D*). A combined expression of PrKX<sub>R283L</sub> and P<sup>0</sup>-site mutants RII $\alpha$ <sub>S99A</sub> or RII $\beta$ <sub>S114A</sub>, lead to BRET signals comparable with RI $\alpha$  and RI $\beta$  wild type holoenzymes (Fig. 2).

<sup>7</sup> M. Diskar and A. Prinz, unpublished data.

**TABLE 1**
**Rate and equilibrium binding constants of PrKX/R and C $\alpha$ /R subunit interaction derived from SPR analyses**

 Concentration series of the respective R subunit (0.5–512 nM) were injected over surfaces containing 200–300 response units covalently immobilized to PrKX, PrKX<sub>R283L</sub>, C $\alpha$ , or C $\alpha$ <sub>L277R</sub> in the presence of ATP/Mg<sup>2+</sup>. The association ( $k_a$ ) and dissociation ( $k_d$ ) rate constants were determined by global fitting assuming a 1:1 Langmuir binding model utilizing BIAevaluation 4.1 (Biacore AB). Equilibrium binding constants ( $K_D$ ) were calculated by dividing  $k_d$  with  $k_a$ .

	RI $\alpha$	RI $\beta$	RII $\alpha$	RII $\beta$	RI $\alpha$ <sub>A99S</sub>	RII $\alpha$ <sub>S99A</sub>
<b>PrKX</b>						
$k^a$ (M <sup>-1</sup> s <sup>-1</sup> )	$2.6 \times 10^5$	$6.9 \times 10^5$			$2.3 \times 10^5$	$2.1 \times 10^4$
$k^d$ (s <sup>-1</sup> )	$2.2 \times 10^{-4}$	$2.8 \times 10^{-3}$			$1.1 \times 10^{-2}$	$4 \times 10^{-3}$
$K^D$ (nM)	0.8	4	~3–4 $\mu$ M	~5–10 $\mu$ M	47	195
<b>PrKX<sub>R283L</sub></b>						
$k^a$ (M <sup>-1</sup> s <sup>-1</sup> )	$5.9 \times 10^5$	$7.9 \times 10^5$	$2 \times 10^5$	$3.2 \times 10^4$	$7.3 \times 10^5$	$5.1 \times 10^4$
$k^d$ (s <sup>-1</sup> )	$5 \times 10^{-4}$	$1.1 \times 10^{-3}$	$5.7 \times 10^{-2}$	$2.0 \times 10^{-2}$	$1.4 \times 10^{-2}$	$1.3 \times 10^{-2}$
$K^D$ (nM)	0.8	1.4	285	650	19	251
<b>C<math>\alpha</math></b>						
$k^a$ (M <sup>-1</sup> s <sup>-1</sup> )	$8.1 \times 10^5$	$2.2 \times 10^6$	$3.1 \times 10^5$	$3.9 \times 10^5$	$8.6 \times 10^5$	$2 \times 10^5$
$k^d$ (s <sup>-1</sup> )	$8 \times 10^{-5}$	$3.8 \times 10^{-4}$	$2.3 \times 10^{-4}$	$3.1 \times 10^{-4}$	$1 \times 10^{-3}$	$4.6 \times 10^{-4}$
$K^D$ (nM)	0.1	0.17	0.77	0.79	1.2	2.3
<b>C<math>\alpha</math><sub>L277R</sub></b>						
$k^a$ (M <sup>-1</sup> s <sup>-1</sup> )	$9.1 \times 10^5$	$2.4 \times 10^6$	$5 \times 10^5$	$3 \times 10^5$	$9.7 \times 10^5$	$1.6 \times 10^5$
$k^d$ (s <sup>-1</sup> )	$1.9 \times 10^{-4}$	$7.8 \times 10^{-4}$	$2.6 \times 10^{-3}$	$1.1 \times 10^{-3}$	$1.4 \times 10^{-3}$	$1 \times 10^{-3}$
$K^D$ (nM)	0.2	0.33	5.2	3.5	1.4	6.2

Using SPR, a  $K_D$  value of 251 nM compared with ~3–4  $\mu$ M (Table 1) translates into a ~12–16-fold increased affinity of PrKX<sub>R283L</sub> and RII $\alpha$ <sub>S99A</sub>. As depicted in Fig. 2, B and C, results of BRET assays employing either RI $\alpha$  or RI $\beta$  in combination with wild type PrKX or PrKX<sub>R283L</sub> display a similar holoenzyme dynamics. As previously shown for RI $\alpha$  wild type holoenzymes with C $\alpha$  or PrKX (15, 16), wild type RI $\beta$  holoenzymes with PrKX and PrKX<sub>R283L</sub> do not respond with complete dissociation upon cAMP elevation in living cells (Fig. 2, B and C). *In vitro*, the affinity of RI $\beta$  and PrKX<sub>R283L</sub> measured by SPR increased by about a factor 3 (Table 1 and Fig. 3B), due to a reduction in the off-rate. The interaction of wild type PrKX with mutant RI $\alpha$  and RI $\beta$  resulted in comparably high BRET values (Fig. 2, B and C and Ref. 15). Introducing a Ser residue at the P<sup>0</sup>-site in both type I R subunits prohibited binding of PrKX. In the case of RI $\alpha$ , but not RI $\beta$ , the negative effect of this mutation was partially compensated by changing Arg-283<sup>PrKX</sup> to Leu (Fig. 2, B and C). This was also reflected by a 2-fold stronger *in vitro* binding of RI $\alpha$ <sub>A99S</sub> to PrKX<sub>R283L</sub> compared with PrKX (Table 1). In a previous study, we showed that interaction of PrKX with an *in vitro* phosphorylated RI $\alpha$ <sub>A99S</sub> protein was completely abolished (15). From this we can conclude that Arg-283<sup>PrKX</sup> located in the  $\alpha$ H- $\alpha$ I loop region prohibits high-affinity binding to and thus functional inhibition of PrKX by wild type RII or mutant RI subunits in living cells.

Initial investigation of a putative ortholog of PrKX from *C. elegans* (F47F2.1b) did not lead to significant interaction with human R subunits in the BRET assay. We therefore reasoned that replacing the Arg at position 324 for Leu in F47F2.1b might stabilize the interaction with R subunits in analogy to human PrKX. This was indeed the case, as we gained interaction of the mutant C subunit with RI $\alpha$  and RI $\beta$  subunits (supplemental Fig. S2A). The PKAC3 protein from *T. brucei* is the only putative PrKX ortholog investigated in this study that does not carry an Arg at the position corresponding to Arg-283<sup>PrKX</sup> but a Pro (Fig. 2A). We therefore investigated the interaction of the protein to R subunits after replacing Pro-254<sup>PKAC3</sup> with Leu. Interestingly, interactions of wild type PKAC3 with either RI $\alpha$  or RI $\beta$  subunits were reduced to background levels upon mutation of

the C subunit, indicating the importance of the Pro residue for holoenzyme formation with this *T. brucei* C subunit (supplemental Fig. S2B).

**Mutation of Leu-277<sup>C $\alpha$</sup>  Influences Holoenzyme Activation—**To test the hypothesis of a central role of Leu277<sup>C $\alpha$</sup> , which corresponds to Arg-283<sup>PrKX</sup>, in maintaining a stable PKA holoenzyme complex, we investigated the consequence of introducing an Arg at position 277 in C $\alpha$  *in vitro* and in living cells. This mutation had no effect on the specific activity of the purified kinase, determined by the coupled spectrophotometric assay (20) ( $20 \pm 1.1$  units/mg, data not shown). We then tested the activation of reconstituted holoenzymes containing wild type and C $\alpha$ <sub>L277R</sub> with four R isoforms *in vitro* (Table 2). Intriguingly, the apparent activation constants ( $K_{act}$ ) of all mutant holoenzymes tested were significantly reduced, in other words, the activation threshold for cAMP is lowered in the mutant holoenzyme complexes under *in vitro* conditions. The effects ranged from a reduction by factor 2 in the case of RI subunits up to factor 4 in the RII $\beta$  containing holoenzyme. These results were obtained with proteins from two independent protein preparations.

Interaction analyses by SPR revealed that the affinity of the C $\alpha$ <sub>L277R</sub> subunit toward R subunits is reduced (Table 1 and Fig. 3, E–H). The effect is again more evident with RII subunits (factor 6.75 for RII $\alpha$ , factor 4.4 for RII $\beta$ ), compared with a factor 2 for RI $\alpha$  and RI $\beta$ . The increased  $K_D$  values were due to faster off-rates with the C $\alpha$ <sub>L277R</sub> compared with wild type C $\alpha$  (Table 1 and Fig. 3, E–H). We then went on to test the interaction of PKA C $\alpha$  as well as C $\alpha$ <sub>L277R</sub> with wild type and mutant human R subunits in living cells using the BRET assay. In accordance to a previous study comparing the PKA-type I $\alpha$  and PKA-type II $\alpha$  holoenzyme dissociations upon cAMP elevation, we observed that RI $\alpha$  or RI $\beta$  containing holoenzymes are less sensitive to activation by cAMP (Ref. 15, and data not shown), in contrast to the RII $\alpha$  and RII $\beta$  containing holoenzymes (Fig. 4, A and B), which readily activate. This almost dominant inhibitory effect of the RI subunits is lost by simple mutation of the autoinhibitory site from a pseudosubstrate to a substrate site (Ref. 15, and data not shown). In contrast, replacing the RII $\alpha$  or RII $\beta$  subunit

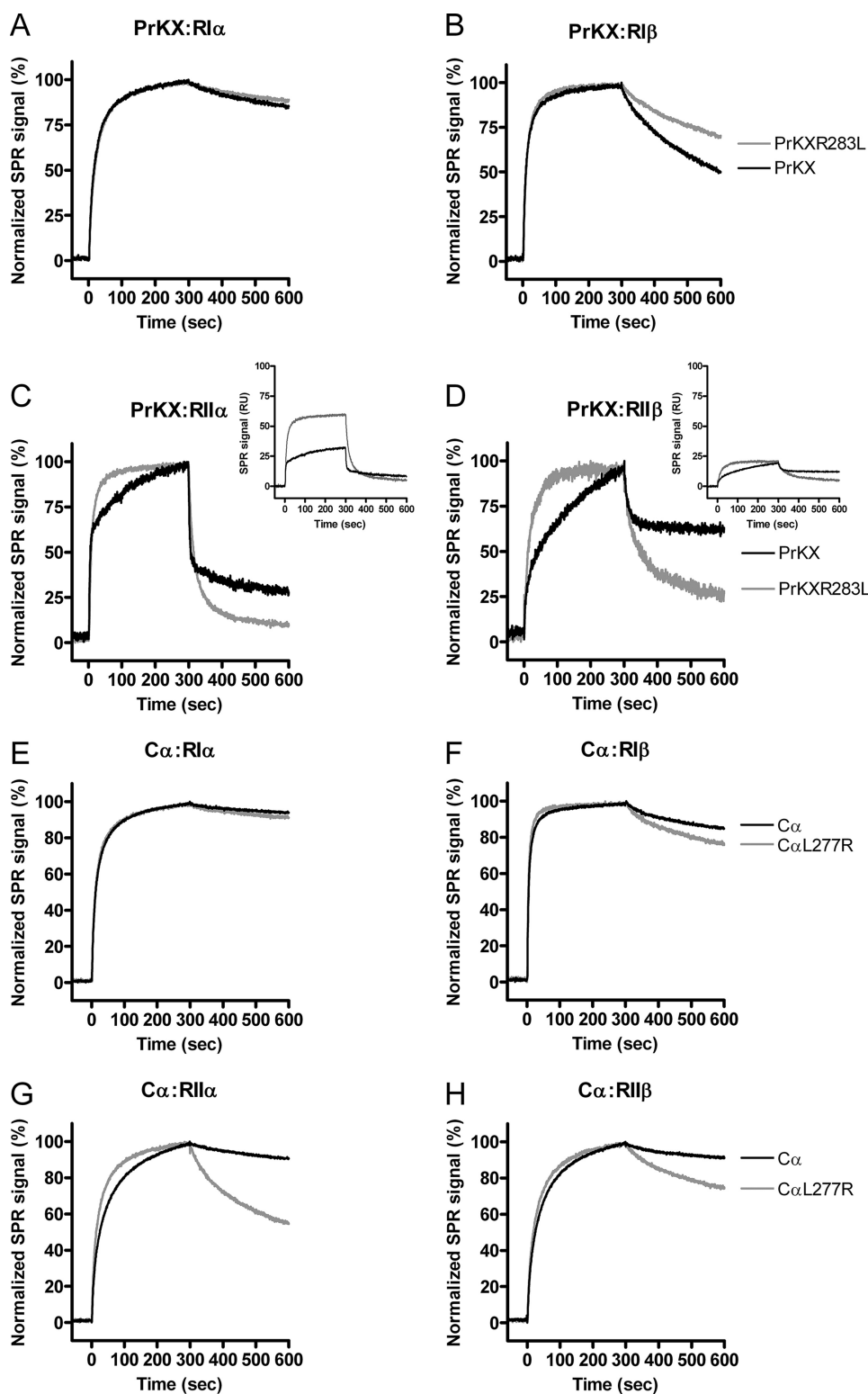


FIGURE 3. Representative SPR sensorgrams of R subunit binding to immobilized His<sub>6</sub>-tagged PrKX, PrKX<sub>R283L</sub>, C $\alpha$ , and C $\alpha$ <sub>L277R</sub>. All C subunits were covalently coupled on Ni<sup>2+</sup>-NTA sensor surfaces. Shown are normalized binding curves, where 128 nM of each RII $\alpha$  (A and E), RII $\beta$  (B and F), RII $\alpha$  (C and G), and RII $\beta$  subunit (D and H) were injected at a flow rate of 30  $\mu$ l/min in running buffer containing ATP/Mg<sup>2+</sup>, except for PrKX, where an injection of 512 nM of the RII $\alpha$ /RII $\beta$  subunits is depicted (C and D). Insets in panels C and D represent original SPR data for the PrKX/RII $\alpha$  and PrKX/RII $\beta$  interactions.

P<sup>0</sup>-site Ser with Ala prohibits a complete activation by cAMP in the context of the living cell (Fig. 4, A and B). Interestingly, this inhibitory effect of the P<sup>0</sup>-site mutation was lost, and [cAMP]<sub>i</sub>

was again able to activate the holoenzymes significantly when the RII $\alpha$ / $\beta$  subunits were combined with the mutant C $\alpha$ <sub>L277R</sub> (Fig. 5). In the case of the PKA type I holoenzymes, mutation of the C subunit  $\alpha$ H- $\alpha$ I loop had no measurable effect on holoenzyme formation or dissociation in living cells (data not shown).

In summary, the mutation of Leu-277 in C $\alpha$  leads to destabilization of the PKA holoenzyme *in vitro*, due to a reduced subunit affinity and activation at lower cAMP concentrations. This effect is stronger when investigating holoenzyme formation with RII subunits, thus resembling the situation in PrKX holoenzymes, which exhibit a strongly reduced binding affinity *in vitro* leading to no significant RII subunit binding *in vivo*. Under steady-state conditions in living cells, mutation of the C subunit at position Leu-277 to Arg has more subtle effects, influencing the stability of RII containing holoenzymes.

**Modeling of the C $\alpha$  Leu-277 to Arg Mutation**—To gain insight in putative structural and regulatory consequences of changing C $\alpha$  Leu-277 to Arg on the interaction network of PKA type II, we modeled the wild type and mutant complexes on the basis of the available experimental structure of the PKA RII $\alpha$ -C $\alpha$  complex (PDB entry code 2QVS (4)). The model was refined by means of MD simulations: 14 ns of MD were performed and root mean square deviations fluctuated at about 3 Å. In the wild type structure, Leu-277<sup>C $\alpha$</sup>  is located in the intersubunit cleft, packed against the side chain of Arg-280<sup>C $\alpha$</sup> , which forms a salt bridge interaction with Glu-208<sup>C $\alpha$</sup>  (40). On the other side of Leu-277<sup>C $\alpha$</sup> , the so called intersubunit interface site 3 (3, 4) includes a salt bridge network of the activation loop and  $\alpha$ A-helix residues formed by Arg-194<sup>C $\alpha$</sup> , Asp-271<sup>brII $\alpha$</sup> , and Arg-245<sup>brII $\alpha$</sup>  (Fig. 5A). This region is crucial for stabilizing the holoenzyme conformation as well as for the allosteric coupling in the PKA holoenzyme. For instance, the Arg-245/Asp-271<sup>brII $\alpha$</sup>  salt bridge plays a key role in coupling the cAMP binding domains

zyme conformation as well as for the allosteric coupling in the PKA holoenzyme. For instance, the Arg-245/Asp-271<sup>brII $\alpha$</sup>  salt bridge plays a key role in coupling the cAMP binding domains

## Intracellular PKA Holoenzyme Regulation

of the R subunit (3, 41). In the complex, the tip of the activation loop of C $\alpha$ , namely residues Lys-192-Gly-193-Arg-194, is packed in the intersubunit interface to form hydrophobic contacts with Ser-264 and Met-267 in bRII $\alpha$  (Fig. 5A). These interactions are observed in the experimental structures and are reproduced in our simulations of the wild type complex. On the contrary, mutating Leu-277<sup>C $\alpha$</sup>  to Arg affects the conformation of the Asp-271<sup>bRII $\alpha$</sup>  side chains, which rotate toward and interact with Arg-277<sup>C $\alpha$</sup>  (Fig. 5B). The interaction network of the site is affected so that the solvent exposition of the residues in the tip of the activation loop increases by about 45 Å<sup>2</sup> in the mutant complex, with respect to the wild type, indicating higher solvation of the intersubunit interface. Although the  $K_D$  values of the wild type *versus* mutant type II $\alpha$  holoenzyme decreased only by a factor of 6.75, still being in the nanomolar range of affinity (Table 1), the theoretical structural analysis supports our experimental data, which showed a decrease in binding affinity of RII subunits to C $\alpha$ <sub>L277R</sub> and a facilitated activation of the mutant PKA holoenzymes.

## DISCUSSION

Phylogenetic analyses performed on the kinase core (8) and the overall sequence of PrKX (supplemental Fig. S1, A and B, and Table S1) indicate that the kinase and its orthologs belong to the family of AGC kinases but are distinct from conventional PKA. Although the kinase core of PrKX shares significant overall homology to PKA C $\alpha$  (~57% identity (8)), other regions,

**TABLE 2**

**Apparent activation constants ( $K_{act}$ ) are reduced in mutant (C $\alpha$ <sub>L277R</sub>) holoenzymes**

Activation constants for cAMP were determined using a spectrophotometric kinase activity assay (20), employing the substrate peptide Kemptide and 20 nM (10 nM for RII $\beta$ ) mutant or wild type holoenzyme per experimental condition. Holoenzymes were formed in a buffer containing Mg<sup>2+</sup> ATP by adding 1.2-fold molar excess of purified R subunits to the C subunits, as indicated, and incubated with a dilution series of cAMP, to obtain  $K_{act}$  values. The data are derived from four experiments, each performed in duplicate. They are given as mean  $\pm$  S.D.

	$K_{act}$ for cAMP ( $\pm$ S.D.)			
	RI $\alpha$	RI $\beta$	RII $\alpha$	RII $\beta$
C $\alpha$	105.5 $\pm$ 7	33.5 $\pm$ 0.7	118 $\pm$ 3	405 $\pm$ 14
C $\alpha$ <sub>L277R</sub>	55 $\pm$ 4	16 $\pm$ 7	53 $\pm$ 5	108 $\pm$ 16

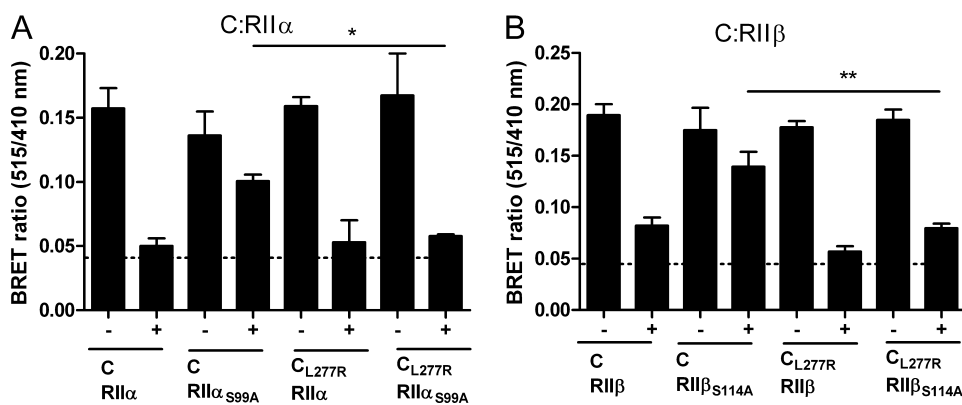


**FIGURE 4. Mutation of C $\alpha$  subunit influences intracellular holoenzyme dynamics.** BRET analyses were carried out as detailed in the legend to Fig. 1. A, plasmids coding for GFP<sup>2</sup>-C $\alpha$  and GFP<sup>2</sup>-C $\alpha$ <sub>L283R</sub> were co-transfected with constructs expressing either RII $\alpha$ -Rluc or RII $\alpha$ <sub>S99A</sub>-Rluc. B, as in A, combined with either RII $\beta$ -Rluc or RII $\beta$ <sub>S114A</sub>-Rluc constructs. Depicted are original BRET values (mean  $\pm$  S.E.) obtained from at least three independent repeats ( $n = 6$  wells; \*\*,  $p < 0.01$ ; \*,  $p < 0.05$ ). +, indicates treatment with forskolin/IBMX; -, indicates mock treatment. The dotted line represents the mean background value.

including the N and C termini (~23 and ~40% identity, respectively) have diverged. The N terminus is the least conserved part, even among PrKX-like kinases. Large insertions, for example, in DdPK2 from *Dictyostelium discoideum* (42, 43), and in DC2 from *D. melanogaster* (33) are characteristic for some PrKX-like kinases (supplemental Fig. S1A). This diversity is reflected in the phylogenetic analysis of the overall sequence (supplemental Fig. S1A), the kinase core, and the C termini of the kinases (not shown), where PKA C subunits are placed in a well resolved group, clearly separated from other kinase families. On the contrary, a PrKX subfamily cannot be as clearly drawn by phylogenetic analysis only. Taking into account the experimental data provided herein, we would like to propose a more conserved PrKX subfamily including vertebrate and insect PrKX and a more extended family, which includes *C. elegans* (F47F2.1b), *T. brucei* (PKAC3), and possibly *D. discoideum* (DdPK2) (supplemental Fig. S1A). Unfortunately, all attempts to express full-length DdPK2 or an N-terminal deletion variant ( $\Delta$ 1–136) for interaction analyses in mammalian cells were unsuccessful (data not shown).

To address the PrKX family experimentally, we focused on its conserved R subunit inhibitory pattern, and we are able to provide evidence that human PrKX, mouse Pkare, *D. melanogaster*  $\Delta$ DC2, and *T. brucei* PKAC3 all share the common feature of a RI over RII subunit preference with respect to autoregulation (Fig. 1). Human PrKY, which lacks the  $\alpha$ H- $\alpha$ I loop, and a mutant *C. elegans* kinase (F47F2.1b<sub>R324L</sub>), bind only to RI $\beta$  when tested with BRET (Fig. 1 and supplemental Fig. S2). By this, we conclude that many if not all kinases of the PrKX family are autoinhibited only by RI subunits, which contain a pseudosubstrate autoinhibitory domain. To substantiate these results, interaction analyses with homologous R subunits have to be performed. Recently, the *D. melanogaster* protein Swiss cheese was identified as a non-canonical R subunit binding to DC2, inhibiting both DC2 and the esterase activity of Swiss cheese mainly in the brain (44). Whether this regulation is conserved in mammalian tissues, awaits experimental evaluation, but this also points to the functional separation of conventional PKA and PrKX-like kinases.

Comprehensive mutational analyses on yeast PKA by Gibbs

*et al.* (41) and x-ray structural analyses (3, 4) suggest that in addition to the active site of the kinase at least two more interaction sites with R subunits are present that, in combination, appear to mediate high-affinity binding of PKA C and R subunits. However, we and others (15, 35, 45) demonstrated that RII subunits, due to autophosphorylation of their inhibitory domain, do not bind with high affinity to the active site cleft of C subunits. It was proposed that binding of the RII $\alpha$  subunit  $\alpha$ B-helix to the  $\alpha$ H- $\alpha$ I loop of the kinase is necessary for high affinity interaction of this R subunit to conventional C subunits (4, 46)

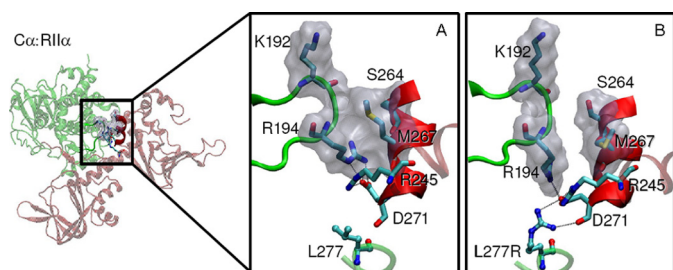


**FIGURE 5. Illustration of the intersubunit interface around Leu-277<sup>Cα</sup> of the PKA type II $\alpha$  holoenzyme.** C $\alpha$  and bRII $\alpha$  subunits are drawn in traces, green and red, respectively. The snapshots were taken at the end of MD simulations. A, wild type PKA C $\alpha$ ; and B, PKA mutant C $\alpha$ <sub>L277R</sub> in complex with bRII $\alpha$ . Residues involved in intersubunit interaction site 3 (4) and discussed in the text are drawn in sticks and are colored by atom type; in particular, Leu277<sup>Cα</sup> (Arg) is drawn in ball and sticks format. For clarity, hydrogen atoms are not shown. Dashed lines indicate salt bridge interactions. Molecular surfaces for Lys-192 and Arg-194 of C $\alpha$ , for Ser-264 and Met-267 of bRII $\alpha$  are drawn in gray.

(Fig. 2). We now show that the inability of RII subunits to regulate PrKX is conferred by a combination of both, the type II R subunit autoinhibitory domain and the PrKX Arg-283 residue located on the  $\alpha$ H- $\alpha$ I loop (Fig. 2). Either mutating the autoinhibitory site in RII to a pseudosubstrate, or changing the Arg-283<sup>PrKX</sup> to the invariant Leu present in conventional C subunits, reconstitutes significant binding of RII subunits to PrKX (Fig. 2). A combination of both mutations did not result in additive, subnanomolar affinities in the SPR assay (Table 1). However, the affinities of RI $\alpha$ /RI $\beta$  interactions with wild type PrKX are already 8- and 24-fold lower compared with the corresponding C $\alpha$  interactions (Table 1). It is conceivable that other non-conserved amino acid substitutions in the kinase core, especially Asp-199<sup>PrKX</sup> (Gly-193<sup>Cα</sup>) or Asn-140<sup>PrKX</sup> (Arg-134<sup>Cα</sup>) might account for the overall lower R subunit binding affinities of PrKX and PrKX<sub>R283L</sub> (8, 41).

Previously, the  $\alpha$ H- $\alpha$ I loop was found to participate in substrate protein binding. A 33-amino acid stretch of the yeast PKA isoform TPK1 (amino acids 298–330), which includes the  $\alpha$ H- $\alpha$ I loop, was sufficient to allow for substrate binding in a yeast two-hybrid assay (47). Moreover, evolutionarily conserved residues in the core of the kinase that link the active site with the C terminus mediate an elevated substrate-binding phenotype, when mutated to alanine, namely Tyr-208<sup>TPK1</sup> (Tyr-164<sup>Cα</sup>), Glu-252<sup>TPK1</sup> (Glu-208<sup>Cα</sup>), Asp-264<sup>TPK1</sup> (Asp-220<sup>Cα</sup>), Trp-266<sup>TPK1</sup> (Trp-222<sup>Cα</sup>), Arg-324<sup>TPK1</sup> (Arg-280<sup>Cα</sup>), and Lys-336/His-338<sup>TPK1</sup> (Lys-292/His-294<sup>Cα</sup>). Mutation of residues Glu-252<sup>TPK1</sup>, Arg-324<sup>TPK1</sup>, and Lys-336/His-338<sup>TPK1</sup> resulted in inactivity of the kinase and prohibited binding to the yeast R subunit (BCY1) (47, 48), which is a substrate for auto-phosphorylation (49).

In our analysis of human C $\alpha$ , we provide strong biochemical evidence for a role of the  $\alpha$ H- $\alpha$ I loop Leu-277<sup>Cα</sup> in stabilizing RII subunit interaction and controlling cAMP-mediated holoenzyme activation. By means of molecular dynamics simulation, we propose that mutation of Leu-277<sup>Cα</sup> to Arg destabilizes the interaction network composed of Asp-271<sup>bRIIα</sup>, Arg-245<sup>bRIIα</sup>, and Arg-194<sup>Cα</sup> (Fig. 5), thus influencing the important interaction of the R subunit  $\alpha$ A-helix with the activation loop (4). PKA activation of the mutant holoenzymes occurred at much lower cAMP concentrations (Table 2), which can be

explained by the fact that Arg-245<sup>bRIIα</sup> (Arg-241<sup>bRIa</sup>) is involved in cAMP binding via Tyr-209<sup>bRIIα</sup> (Glu-200<sup>bRIa</sup>) (4, 50). Finally, Leu-277<sup>Cα</sup> could be involved in stabilizing the Arg-245/Asp-271<sup>bRIIα</sup> (Arg-241/Asp-267<sup>bRIa</sup>) salt bridge, which breaks upon cAMP binding, followed by the major collapse of the  $\alpha$ B/C helix and subsequent holoenzyme dissociation (3, 4, 51). In summary, our work supports a critical involvement of the  $\alpha$ H- $\alpha$ I loop in autoregulation of PrKX-like kinases (Arg-283<sup>PrKX</sup>), in stabilizing PKA type II holoenzymes (Leu-277<sup>Cα</sup>), and in proper allosteric signal propagation in PKA (Leu-277<sup>Cα</sup>), besides the previously recognized role of this region in substrate recognition (47, 48) and in stabilizing the active conformation of the kinase via the universally conserved Arg-280<sup>Cα</sup> residue (40, 52).

*Acknowledgment*—We acknowledge the help of Dr. Martina Rex with phylogenetic analyses.

## REFERENCES

- Herberg, F. W., Taylor, S. S., and Dostmann, W. R. (1996) *Biochemistry* **35**, 2934–2942
- Vigil, D., Blumenthal, D. K., Taylor, S. S., and Trewella, J. (2006) *J. Mol. Biol.* **357**, 880–889
- Kim, C., Cheng, C. Y., Saldanha, S. A., and Taylor, S. S. (2007) *Cell* **130**, 1032–1043
- Wu, J., Brown, S. H., von Daake, S., and Taylor, S. S. (2007) *Science* **318**, 274–279
- Brown, S. H., Wu, J., Kim, C., Alberto, K., and Taylor, S. S. (2009) *J. Mol. Biol.* **393**, 1070–1082
- Schiebel, K., Winkelmann, M., Mertz, A., Xu, X., Page, D. C., Weil, D., Petit, C., and Rappold, G. A. (1997) *Hum. Mol. Genet.* **6**, 1985–1989
- Skalhegg, B. S., and Tasken, K. (2000) *Front. Biosci.* **5**, D678–693
- Li, X., Li, H. P., Amsler, K., Hyink, D., Wilson, P. D., and Burrow, C. R. (2002) *Proc. Natl. Acad. Sci. U.S.A.* **99**, 9260–9265
- Junttila, I., Bourette, R. P., Rohrschneider, L. R., and Silvennoinen, O. (2003) *J. Leukocyte Biol.* **73**, 281–288
- Semizarov, D., Glesne, D., Laouar, A., Schiebel, K., and Huberman, E. (1998) *Proc. Natl. Acad. Sci. U.S.A.* **95**, 15412–15417
- Li, X., Burrow, C. R., Polgar, K., Hyink, D. P., Gusella, G. L., and Wilson, P. D. (2008) *Biochim. Biophys. Acta* **1782**, 1–9
- Li, X., Hyink, D. P., Polgar, K., Gusella, G. L., Wilson, P. D., and Burrow, C. R. (2005) *J. Am. Soc. Nephrol.* **16**, 3543–3552
- Li, X., Hyink, D. P., Radbill, B., Sudol, M., Zhang, H., Zheleznova, N. N., and Wilson, P. D. (2009) *Kidney Int.* **76**, 54–62
- Zimmermann, B., Chiorini, J. A., Ma, Y., Kotin, R. M., and Herberg, F. W. (1999) *J. Biol. Chem.* **274**, 5370–5378
- Diskar, M., Zenn, H. M., Kaupisch, A., Prinz, A., and Herberg, F. W. (2007) *Cell. Signal.* **19**, 2024–2034
- Prinz, A., Diskar, M., Erlbruch, A., and Herberg, F. W. (2006) *Cell. Signal.* **18**, 1616–1625
- Prinz, A., Diskar, M., and Herberg, F. W. (2006) *ChemBioChem* **7**, 1007–1012
- Gesellchen, F., Prinz, A., Zimmermann, B., and Herberg, F. W. (2006) *Eur. J. Cell Biol.* **85**, 663–672
- Bertinetti, D., Schweinsberg, S., Hanke, S. E., Schwede, F., Bertinetti, O., Drewianka, S., Genieser, H. G., and Herberg, F. W. (2009) *BMC Chem. Biol.* **9**, 3
- Cook, P. F., Neville, M. E., Jr., Vrana, K. E., Hartl, F. T., and Roskoski, R., Jr. (1982) *Biochemistry* **21**, 5794–5799
- Berrera, M., Pantano, S., and Carloni, P. (2006) *Biophys. J.* **90**, 3428–3433
- Berrera, M., Pantano, S., and Carloni, P. (2007) *J. Phys. Chem. B* **111**, 1496–1501
- Lindahl, E., Hess, B., and van der Spoel, D. (2001) *J. Mol. Model.* **7**, 306–317



## Intracellular PKA Holoenzyme Regulation

24. Ponder, J. W., and Case, D. A. (2003) *Adv. Protein Chem.* **66**, 27–85
25. Jorgensen, W., Chandrasekhar, J., Madura, J., Impey, R., and Klein, M. (1983) *J. Chem. Phys.* **79**, 926–935
26. Hess, B., Bekker, H., Berendsen, H., and Fraaije, J. (1997) *J. Comput. Chem.* **18**, 1463–1472
27. Sagui, C., and Darden, T. A. (1999) *Annu. Rev. Biophys. Biomol. Struct.* **28**, 155–179
28. Berendsen, H., Postma, J., Vangunsteren, W., Dinola, A., and Haak, J. (1984) *J. Chem. Phys.* **81**, 3684–3690
29. Eisenhaber, F., Lijnzaad, P., Argos, C., Sander, C., and Scharf, M. (1995) *J. Comput. Chem.* **16**, 273–284
30. Berrera, M., Cattaneo, A., and Carloni, P. (2006) *Biophys. J.* **91**, 2063–2071
31. Blaschke, R. J., Monaghan, A. P., Bock, D., and Rappold, G. A. (2000) *Genomics* **64**, 187–194
32. Li, W., Yu, Z. X., and Kotin, R. M. (2005) *J. Histochem. Cytochem.* **53**, 1003–1009
33. Meléndez, A., Li, W., and Calderon, D. (1995) *Genetics* **141**, 1507–1520
34. Berriman, M., Ghedin, E., Hertz-Fowler, C., Blandin, G., Renaud, H., Bartholomeu, D. C., Lennard, N. J., Caler, E., Hamlin, N. E., Haas, B., Böhm, U., Hannick, L., Aslett, M. A., Shallom, J., Marcello, L., Hou, L., Wickstead, B., Alsmark, U. C., Arrowsmith, C., Atkin, R. J., Barron, A. J., Bringaud, F., Brooks, K., Carrington, M., Cherevach, I., Chillingworth, T. J., Churcher, C., Clark, L. N., Corton, C. H., Cronin, A., Davies, R. M., Doggett, J., Djikeng, A., Feldblyum, T., Field, M. C., Fraser, A., Goodhead, I., Hance, Z., Harper, D., Harris, B. R., Hauser, H., Hostetler, J., Ivens, A., Jagels, K., Johnson, D., Johnson, J., Jones, K., Kerhornou, A. X., Koo, H., Larke, N., Landfear, S., Larkin, C., Leech, V., Line, A., Lord, A., Macleod, A., Mooney, P. J., Moule, S., Martin, D. M., Morgan, G. W., Mungall, K., Norbertczak, H., Ormond, D., Pai, G., Peacock, C. S., Peterson, J., Quail, M. A., Rabinowitsch, E., Rajandream, M. A., Reitter, C., Salzberg, S. L., Sanders, M., Schobel, S., Sharp, S., Simmonds, M., Simpson, A. J., Tallon, L., Turner, C. M., Tait, A., Tivey, A. R., Van Aken, S., Walker, D., Wanless, D., Wang, S., White, B., White, O., Whitehead, S., Woodward, J., Wortman, J., Adams, M. D., Embley, T. M., Gull, K., Ullu, E., Barry, J. D., Fairlamb, A. H., Opperdoes, F., Barrell, B. G., Donelson, J. E., Hall, N., Fraser, C. M., Melville, S. E., and El-Sayed, N. M. (2005) *Science* **309**, 416–422
35. Martin, B. R., Deerinck, T. J., Ellisman, M. H., Taylor, S. S., and Tsien, R. Y. (2007) *Chem. Biol.* **14**, 1031–1042
36. Viste, K., Kopperud, R. K., Christensen, A. E., and Døskeland, S. O. (2005) *J. Biol. Chem.* **280**, 13279–13284
37. Dalton, G. D., and Dewey, W. L. (2006) *Neuropeptides* **40**, 23–34
38. Hanks, S. K. (2003) *Genome Biol.* **4**, 111
39. Yang, J., Kennedy, E. J., Wu, J., Deal, M. S., Pennypacker, J., Ghosh, G., and Taylor, S. S. (2009) *J. Biol. Chem.* **284**, 6241–6248
40. Johnson, D. A., Akamine, P., Radzio-Andzelm, E., Madhusudan, M., and Taylor, S. S. (2001) *Chem. Rev.* **101**, 2243–2270
41. Gibbs, C. S., Knighton, D. R., Sowadski, J. M., Taylor, S. S., and Zoller, M. J. (1992) *J. Biol. Chem.* **267**, 4806–4814
42. Anjard, C., Etchebehere, L., Pinaud, S., Véron, M., and Reymond, C. D. (1993) *Biochemistry* **32**, 9532–9538
43. Etchebehere, L. C., Van Bemmelen, M. X., Anjard, C., Traincard, F., Assemat, K., Reymond, C., and Véron, M. (1997) *Eur. J. Biochem.* **248**, 820–826
44. Bettencourt da Cruz, A., Wentzell, J., and Kretzschmar, D. (2008) *J. Neurosci.* **28**, 10885–10892
45. Rubin, C. S., Erlichman, J., and Rosen, O. M. (1972) *J. Biol. Chem.* **247**, 36–44
46. Anand, G. S., Hotchko, M., Brown, S. H., Ten Eyck, L. F., Komives, E. A., and Taylor, S. S. (2007) *J. Mol. Biol.* **374**, 487–499
47. Deminoff, S. J., Ramachandran, V., and Herman, P. K. (2009) *Genetics* **182**, 529–539
48. Deminoff, S. J., Howard, S. C., Hester, A., Warner, S., and Herman, P. K. (2006) *Genetics* **173**, 1909–1917
49. Toda, T., Cameron, S., Sass, P., Zoller, M., Scott, J. D., McMullen, B., Hurwitz, M., Krebs, E. G., and Wigler, M. (1987) *Mol. Cell Biol.* **7**, 1371–1377
50. Symcox, M. M., Cauthron, R. D., Ogreid, D., and Steinberg, R. A. (1994) *J. Biol. Chem.* **269**, 23025–23031
51. Gullingsrud, J., Kim, C., Taylor, S. S., and McCammon, J. A. (2006) *Structure* **14**, 141–149
52. Steichen, J. M., Iyer, G. H., Li, S., Saldanha, S. A., Deal, M. S., Woods, V. L., Jr., and Taylor, S. S. (2010) *J. Biol. Chem.* **285**, 3825–3832